TSC22D2 interacts with PKM2 and inhibits cell growth in colorectal cancer

FANG LIANG[1-3], QIAO LI[1-3], XIAYU LI[3], ZHENG LI[1-3], ZHAOJIAN GONG[2,4], HAO DENG[3], BO XIANG[1-3], MING ZHOU[1-3], XIAOLING LI[1-3], GUIYUAN LI[1-3], ZHAOYANG ZENG[1-3] and WEI XIONG[1-3]

[1]Hunan Key Laboratory of Translational Radiation Oncology, Hunan Cancer Hospital and The Affiliated Cancer Hospital of Xiangya School of Medicine, [2]The Key Laboratory of Carcinogenesis of The Chinese Ministry of Health and The Key Laboratory of Carcinogenesis and Cancer Invasion of The Chinese Ministry of Education, Cancer Research Institute, [3]Hunan Key Laboratory of Nonresolving Inflammation and Cancer, Disease Genome Research Center, The Third Xiangya Hospital, [4]Department of Oral and Maxillofacial Surgery, The Second Xiangya Hospital, Central South University, Changsha, Hunan, P.R. China

Received March 23, 2016; Accepted May 16, 2016

DOI: 10.3892/ijo.2016.3599

Abstract. We previously identified TSC22D2 (transforming growth factor β-stimulated clone 22 domain family, member 2) as a novel cancer-associated gene in a rare multi-cancer family. However, its role in tumor development remains completely unknown. In this study, we found that TSC22D2 was significantly downregulated in colorectal cancer (CRC) and that TSC22D2 overexpression inhibited cell growth. Using a co-immunoprecipitation (co-IP) assay combined with mass spectrometry analysis to identify TSC22D2-interacting proteins, we demonstrated that TSC22D2 interacts with pyruvate kinase isoform M2 (PKM2). These findings were confirmed by the results of immunoprecipitation and immunofluorescence assays. Moreover, overexpression of TSC22D2 reduced the level of nuclear PKM2 and suppressed cyclin D1 expression. Collectively, our study reveals a growth suppressor function of TSC22D2 that is at least partially dependent on the TSC22D2-PKM2-cyclinD1 regulatory axis. In addition, our data provide important clues that might contribute to future studies evaluating the role of TSC22D2.

Correspondence to: Dr Zhaoyang Zeng and Dr Wei Xiong, Hunan Key Laboratory of Translational Radiation Oncology, Hunan Cancer Hospital and The Affiliated Cancer Hospital of Xiangya School of Medicine, Cancer Research Institute, Central South University, Changsha, Hunan 410013, P.R. China
E-mail: zengzhaoyang@csu.edu.cn
E-mail: xiongwei@csu.edu.cn

Abbreviations: TSC22D2, TSC22 domain family member 2; PKM2, pyruvate kinase isoform M2; CRC, colorectal cancer

Key words: TSC22 domain family member 2, colorectal cancer, pyruvate kinase isoform M2, cyclin D1, cell growth

Introduction

In a previous study, we performed a genome-wide linkage analysis of 24 core family members in a rare multi-cancer family. The family included 103 members spanning six generations, and 15 members had been diagnosed with various tumor types, including colorectal cancer (CRC), breast cancer, endometrial carcinoma and gastric cancer. The disease susceptibility locus in this family was mapped to chromosome 3q24-26. A novel mutant in the TSC22D2 gene located in chromosome band 3q24-26 co-segregated with the cancer phenotype, as demonstrated by exome sequencing (1).

TSC22D2 is a member of the TSC-22 domain family comprising putative transcription factors that are characterized by a carboxy-terminal leucine zipper and an adjacent TSC-box. However, there are few studies describing TSC22D2, and its role in tumor development remains largely unknown.

Accumulating evidence shows that many TSC22D2 family proteins interact with other proteins to form macromolecular complexes and are involved in a broad range of biological processes. For instance, TSC22D1 (referred as TSC-22) can suppress tumor growth by binding to p53 (2) and can enhance TGF-β signaling by associating with Smad4 (3); TSC22D3 (usually called GILZ) plays multiple biological functions dependent on its interaction with other proteins, including NF-κB, Ras and p53 (4-6). Accordingly, the identification of the TSC22D2-associated proteins or macromolecular complexes is important to precisely understand the underlying mechanism of TSC22D2 in human carcinogenesis.

In this study, we investigated the role of TSC22D2 in colorectal cancer, the most common malignancy in the multi-cancer family. We found TSC22D2 was significantly downregulated in CRC. Further functional study showed that TSC22D2 overexpression can inhibit CRC cell growth. To precisely define the underlying mechanism by which TSC22D2 influenced CRC cell growth, we used co-immunoprecipitation (co-IP) and mass spectrometry approaches to identify the proteins or macromolecular complexes that

interact with TSC22D2, and gained 142 candidate TSC22D2-binding proteins that were associated with a variety of cellular processes. Moreover, we determined that TSC22D2 physically associates with pyruvate kinase isoform M2 (PKM2), a glycolytic enzyme reported to be associated with the growth and survival of multiple cancer cell types (7-9), and demonstrated that TSC22D2 overexpression reduces nuclear PKM2 levels and represses the expression of cyclin D1 (a downstream target gene of nuclear PKM2).

Materials and methods

CRC samples. Surgical cancer tissue specimens and adjacent normal mucosa (≥5 cm away from the tumor margins) were obtained from 14 patients with colorectal cancer who had undergone surgery at the Third Xiangya Hospital of Central South University. Informed written consent was obtained from each patient, and the research protocols were approved by the Medical Ethics Committee of Xiangya Medical College. No patients had received preoperative adjuvant therapy. After collection, all tissue samples were immediately frozen in liquid nitrogen until use.

Plasmid construction. The full length TSC22D2 gene was cloned into the pIRESneo3-Flag vector with *Nhe*I and *Stu*I (Takara, Dalian, China) sites. The TSC22D2 gene was amplified using the following primers: TSC22D2 sense primer (5'-ACG TGCTAGCGCCACCATGTCCAAGATGCCGGCCAA-3'), TSC22D2 anti-sense primer (5'-ACTGAGGCCTTTATGCTG AGGAGACATTCG-3'). Full-length PKM2 was generously provided by Professor Xianghuo He (Shanghai Medical College, Fudan University, Shanghai, China) and has been previously described (10).

Cell lines and cell culture. The SW480 (human colorectal carcinoma) and HEK293 (human embryonic kidney) cell lines were cultured in Dulbecco's modified Eagle's medium (Life Technologies, Grand Island, NY, USA) with 10% fetal bovine serum (FBS) supplemented with 100 U/ml penicillin and 100 mg/ml streptomycin. The HeLa human cervical carcinoma cells were grown in 1640 medium (Life Technologies) supplemented with 10% FBS, 100 U/ml penicillin and 100 mg/ml streptomycin.

Cells were transfected using the Lipofectamine 3000 reagent (Life Technologies) according to the manufacturer's instructions. HEK293, SW480 and HeLa cells stably expressing Flag-tagged TSC22D2 (Flag-TSC22D2) or the control vector (Flag-NC) were obtained by puromycin (600-1,000 ng/ml) (Life Technologies) selection for one month. All cells were maintained under standard culture conditions (37˚C, 5% CO_2).

RNA isolation and quantitative real-time PCR. Total RNAs were isolated using the TRIzol reagent (Invitrogen, Carlsbad, CA, USA), and were converted to cDNA using the GoScript™ Reverse Transcription System (Promega, Madison, WI, USA) according to the manufacturer's instructions. All real-time PCR reactions were performed with SYBR Green (Takara) using the Bio-Rad CFX Connect Real-Time system (Bio-Rad, Hercules, CA, USA). The following PCR program was used: denaturation at 95˚C for 30 sec, followed by 40 cycles consisting of denaturation at 95˚C for 5 sec, annealing at 60˚C for 30 sec, and extension at 72˚C for 30 sec. A melting curve analysis was applied to assess the specificity of the amplified PCR products. The amount of each target gene was quantified by the comparative C_T method using GAPDH as the normalization control. The following primers were synthesized from Life Technologies and used to amplify TSC22D2, CCND1 and GAPDH: TSC22D2 forward primer (5'-TGAT GGTGATGAAGACAGTGC-3'), TSC22D2 reverse primer (5'-GGGTTGGGAGTTGGGATAAT-3'); CCND1 forward primer (5'-CAACCTCCTCAACGACC-3'), CCND1 reverse primer (5'-CTTCTGTTCCTCGCAGAC-3'); GAPDH forward primer (5'-AACGGATTTGGTCGTATTGG-3'), GAPDH reverse primer (5'-TTGATTTTGGAGGGATCTCG-3'). All experiments were carried out in triplicate.

Total protein, subcellular fractionation and western blot analysis. Nuclear and cytosolic extracts were fractionated using the NE-PER nuclear and cytoplasmic extraction kit (Thermo Scientific, Bremen, Germany) according to the manufacturer's protocol. To isolate total protein, cells were harvested by scraping and transferred to SDS sample buffer supplemented with a protease inhibitor cocktail and the PhosSTOP phosphatase inhibitor (Roche, Pleasanton, CA, USA). Equal levels of protein from the samples were separated using SDS-PAGE gel electrophoresis and transferred to a PVDF membrane (Millipore Corp., Billerica, MA, USA). The membrane was blocked with PBST containing 5% skim milk for 1 h and then incubated overnight with the indicated primary antibodies at 4˚C. The membrane was washed three times in PBST and subsequently incubated with an HRP-conjugated secondary antibody for 2 h at 37˚C. The membranes were stripped of the primary antibodies and re-probed with additional antibodies as necessary. Bound antibodies were visualized using the enhanced chemiluminescence kit (Millipore).

The following antibodies were used in this study: monoclonal mouse anti-Flag (F1804, Sigma, St. Louis, MO, USA), anti-HA (H3663, Sigma), polyclonal rabbit anti-human TSC22D2 (AV39137, Sigma), polyclonal rabbit anti-human PKM2 (Cell Signaling, Danvers, MA, USA) and anti-CCND1 (Cell Signaling). An antibody against GAPDH (Cell Signaling) served as an endogenous control for equal loading, and anti-H3 (Beyotime, China) served as a nuclear control.

Cell proliferation assays. Cell proliferation was measured by counting viable cells using the Z2 Particle Counter and Size Analyzer Beckman Coulter (Miami, FL, USA). Briefly, SW480 and HeLa cells stably expressing Flag-tagged TSC22D2 (Flag-TSC22D2) or the control vector (Flag-NC) were seeded at $1.2x10^4$ cells per well in 24-well plates in quadruplicate, the number of viable cells in each well was measured at 0, 1, 2, 3, 4 and 5 days.

Colony formation assays. For the colony formation assays, SW480 and HeLa cells were seeded in a 6-well plate at a density of 500 and 200 cells per well respectively, and incubated at 37˚C with 5% CO_2 for 2 weeks. The medium was changed every 3-4 days. At the end of the incubation, the medium was removed, and the cells were washed twice with PBS, fixed with 4% paraformaldehyde for 20 min, stained

with crystal violet for 30 min at room temperature, washed and imaged. Colonies of >50 cells were identified using an inverted microscope (Olympus IX50; Olympus Corp., Tokyo, Japan) and counted.

Flow cytometry cell cycle assays. SW480 and HeLa stable cells were plated at a density of $4x10^5$ cells per well in 6-well plates and cultured in medium without serum (starvation treatment) for 12 h to synchronize cell cycle progression. Cells were incubated in serum-containing growth medium for an additional 24-36 h and subsequently trypsinized, washed, fixed with 70% ice cold ethanol overnight at 4˚C. DNA was stained by incubating the cells in PBS containing PI (50 μg/ml) and RNase A (50 μg/ml). The cell cycle distribution was determined by flow cytometric analysis using a MoFlo™ XDP High-Performance Cell Sorter (Beckman Coulter, Brea, CA, USA) and the data were analyzed using Summit v.5.2 software.

Co-immunoprecipitation (co-IP) assays. HEK293 Flag-NC, HEK293 Flag-TSC22D2, SW480 Flag-NC, SW480 Flag-TSC22D2 stably transfected cells and HEK293T cells transiently cotransfected with Flag-TSC22D2 and HA-PKM2 were seeded in 100-mm dishes. The cells were lysed in modified lysis buffer (50 mM Tris-HCl pH 7.5, 100 mM NaCI, 50 mM NaF, 1 mM Na_3VO_4, 30 mM sodium pyrophosphate, 0.5% NP-40 and 0.5 mM PMSF (Sigma) supplemented with an EDTA-free protease inhibitor cocktail (Roche). Lysates were incubated with 5 μg of primary antibody overnight at 4˚C. Then, 40 μl of a 1:1 slurry of protein A/G Plus-agarose (Santa Cruz, CA, USA) and a specific antibody were added to the cells for ≥4 h at 4˚C. The immunoprecipitates were washed four times with lysis buffer and boiled with sample loading buffer and then analyzed by western blotting.

Mass spectrometry. Proteins were resolved on a 10% polyacrylamide gel, stained with Coomassie Brilliant Blue (R250) and subjected to mass spectrometry. Briefly, the stained SDS-PAGE gels were scanned, and stained bands were excised, cut into small (<1 mm^3) pieces and washed three times by repetitive dehydration and hydration with acetonitrile and ammonium bicarbonate, respectively. Proteins were in-gel reduced in the presence of 25 mM DTT and 25 mM NH_4HCO_3 for 1 h at 56˚C, immediately alkylated using 50 mM IAA and 25 mM NH_4HCO_3 for 30 min at room temperature in the dark and digested overnight at 37˚C with 5 μg of trypsin in 25 mM NH_4HCO_3. Digested peptides were recovered, dried and resuspended in 50% CAN and 0.1% TFA. The peptide mixture was analyzed by nano-liquid chromatography-tandem mass spectrometry using an LTQ Velos-Orbitrap MS (Thermo Scientific, Waltham, MA, USA) coupled to an Ultimate RSLC nano-LC system (Dionex). Briefly, Raw MS data files were processed using the Proteome Discoverer v.1.4 (Thermo Scientific). Processed files were searched against the Swiss-Prot human database using the Sequest HT search engine. Mass tolerances for precursor and fragment ions were set to 10 ppm and 0.8 Da, respectively, in the database searches. Peptide identification with false discovery rates <1% (q-value <0.01) were discarded.

Immunofluorescence. TSC22D2, HEK293, SW480 and HeLa cells grown on culture slides were maintained in a 35-mm dish. After cultured for 24 h, the cells were washed with phosphate-buffered saline (PBS), fixed with 4% paraformaldehyde in PBS for 10 min, permeabilized with 0.25% Triton X-100 for 30 min and blocked in 5% bovine serum albumin (BSA) for 1 h at room temperature. Fixed cells were then incubated with rabbit anti-human TSC22D2 antibody (1:1,000) at 4˚C overnight, washed three times in PBS and stained with Alexa Fluor 488 donkey anti-rabbit IgG (Invitrogen, 1:1,000) for 2 h in the dark at room temperature. The cells were then incubated with DAPI to stain the nuclei and visualized using a confocal laser scanning microscope (Olympus Corp.).

For the colocalization assays, HEK293T transfected with Flag-TSC22D2 and HA-PKM2 were incubated with the anti-Flag mouse monoclonal antibody (1:1,000) and the anti-PKM2 rabbit monoclonal antibody (1:1,000) at 4˚C overnight and subsequently stained with Alexa Fluor 488 donkey anti-mouse IgG (Invitrogen, 1:1,000) and Alexa Fluor 594 donkey anti-rabbit IgG (Invitrogen, 1:1,000) for 2 h at room temperature. After incubation with DAPI to stain the nuclei, the cells were visualized using a confocal laser scanning microscope (UltraView Vox; Perkin-Elmer, Waltham, MA, USA).

Statistical analysis. The experiments were repeated at least three times. All data are presented as the mean ± standard deviation. Paired Student's t-test (two-tailed) and unpaired Student's t-test (two-tailed) were performed to compare the means of two samples unless otherwise indicated. A p-value <0.05 was considered statistically significant. All statistical analyses were performed using the GraphPad Prism software (Graphpad Software, Inc.).

Results

Expression of TSC22D2 is decreased in colorectal cancer samples. We focused on human colorectal cancer in this study because it was the most frequent malignancy in the multi-cancer family. We first evaluated the expression of TSC22D2 transcripts in colorectal cancer by interrogating the public gene expression GEO databases (GSE8671, GSE32323 and GSE24514) and found that the expression of TSC22D2 was lower in human colorectal cancer samples than in non-tumor samples (Fig. 1A). To confirm these observations, the expression of TSC22D2 was evaluated in 14 pairs of human CRC samples (primary tumor tissues and paired adjacent non-tumor tissues). TSC22D2 expression was reduced in 13 of 14 (92.9%) of colorectal tumors compared with the paired adjacent non-tumor tissues (Fig. 1B, p=0.015), consistent with the data provided by the GEO database. These results suggest that TSC22D2 plays a suppressor role in CRC tumorigenesis.

TSC22D2 suppresses CRC cell growth. To investigate the function of TSC22D2 in colorectal cancer, the full-length TSC22D2 gene tagged with three Flag tags was cloned into the pIRESneo3 plasmid and stably transfected into SW480 and HeLa cells. The expression of TSC22D2 was confirmed by qRT-PCR and western blot analysis (Fig. 2A). Immunofluorescence assays demonstrated that TSC22D2 predominantly localized to the cytoplasm under steady state conditions (Fig. 2B). Cell proliferation assays and clone

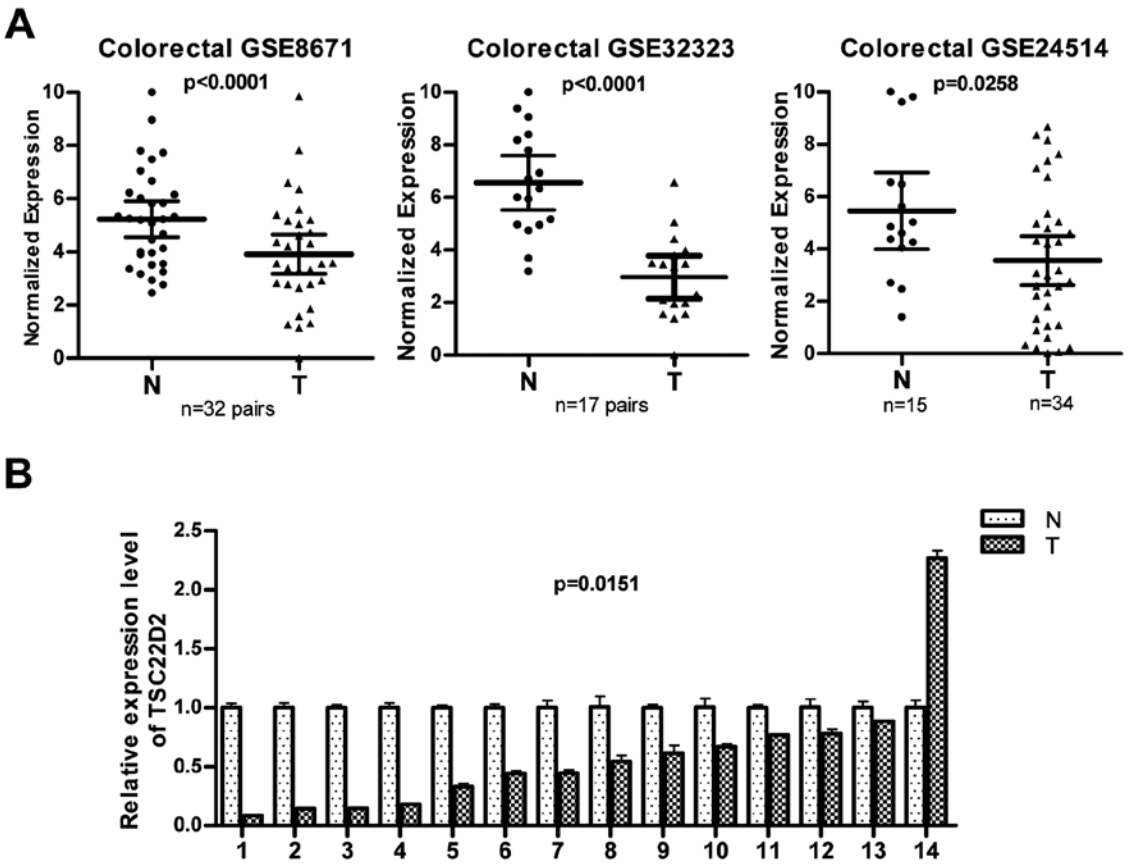

Figure 1. Expression of TSC22D2 is reduced in colorectal cancer tissue. (A) The TSC22D2 mRNA expression data in CRC and control normal tissue samples were extracted from the GEO datasets GSE8671, GSE32323 and GSE24514. TSC22D2 was significantly downregulated in CRC samples. (B) TSC22D2 expression was further confirmed in colorectal tumor tissue and paired adjacent non-tumor tissue samples using real-time PCR.

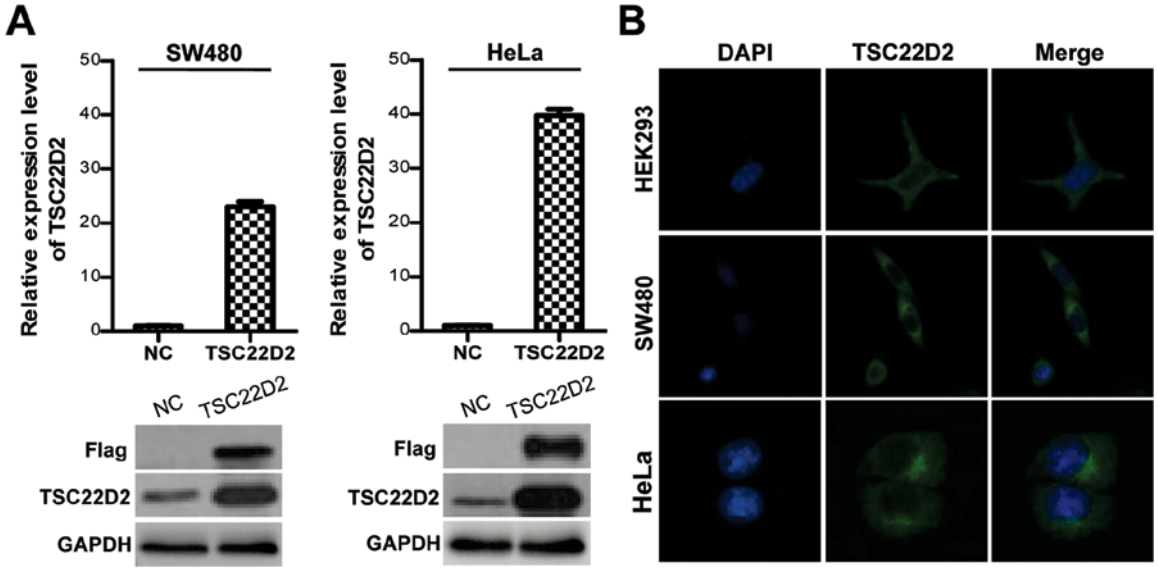

Figure 2. Verification of stable TSC22D2-overexpression cell lines. (A) SW480 and HeLa cells were transfected with the TSC22D2 overexpression vector. The expression of TSC22D2 in the cells was validated by qRT-PCR and western blot analysis. (B) Immunofluorescence assays revealed that the TSC22D2 protein primarily localized to the cell cytoplasm in HEK293, SW480 and HeLa cells.

formation assays were conducted to investigate the effect of TSC22D2 on cell proliferation. TSC22D2-overexpressing cells exhibited a significantly slower growth rate (Fig. 3A) and a reduced number of clones (Fig. 3B) compared with control cells, indicating that TSC22D2 functions as a suppressor in CRC cell growth. Furthermore, flow cytometry (FCM) revealed that TSC22D2 induced a substantial increase in the proportion of cells at the G0/G1 phase and a concomitant

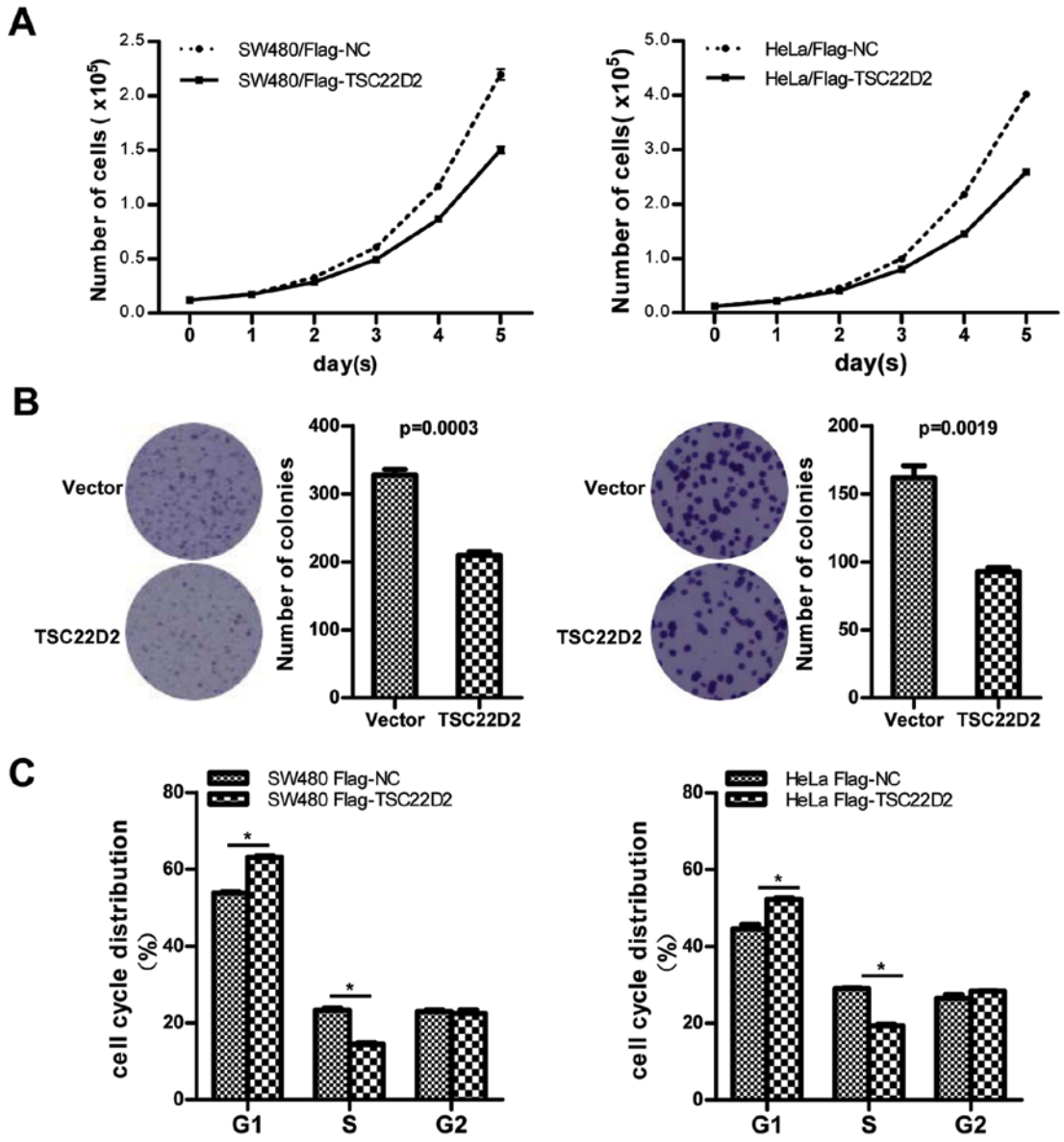

Figure 3. TSC22D2 suppresses cancer cell growth. (A) Growth curves generated from the results of the cell proliferation assays indicated that TSC22D2 overexpression inhibited proliferation in SW480 and HeLa cells. (B) A reduced number of clones was observed in SW480 and HeLa cells overexpressing TSC22D2A. Representative images show a partial view of colony growth after 2 weeks. The data are presented as the mean ± SD of three independent cultures. (C) Flow cytometry analysis of cell cycle progression demonstrated that TSC22D2 induced cell cycle arrest at the G0/G1 phase in SW480 and HeLa cells. *p<0.05.

decrease in the proportion of cells at the S phase of the cell cycle (Fig. 3C). These results indicate that TSC22D2 induces cell cycle arrest at the G0/G1 phase.

Identification of TSC22D2 binding partners. To explore the underlying mechanism by which TSC22D2 exerts its tumor-suppressive function, we performed co-IP assays (Fig. 4A) and LC-MS/MS analysis (Fig. 4B) in SW480 and HEK293 cells stably transfected with TSC22D2. We identified 90 and 79 candidate proteins in SW480 and HEK293 samples, respectively (Fig. 4C). There were 27 overlapping results for proteins associated with metabolism (PKM2, ATP5A1, LDH and ENO1), stress response and inflammation (STK39, HSPD1, HSP90AA1 and HSP90AB1), cell proliferation (NRBP1, PKM2, YWHAQ, LDHB, PCNA and PHB2), apoptosis (HSPD1, CAPN1, DNAJA1, HSP90AA1 and RPS3) and migration/metastasis (YWHAQ, HSPD1 and PHB2) between the 2 cell lines (Fig. 4D and Table I). These findings suggest that TSC22D2 plays a role in these biological pathways in cancer cells.

TSC22D2 physically associates with PKM2. We selected PKM2, a glycolytic enzyme that catalyzes the conversion of phosphoenopyruvate (PEP) and ADP to pyruvate and ATP for further analysis due to its relatively high mass spectrometry score and its previously reported role in cancer cell growth and survival (7-9).

The interaction between PKM2 and TSC22D2 was further confirmed by IP analysis of HEK293T cells transfected with HA-tagged PKM2 and Flag-tagged TSC22D2 (Fig. 5A). To

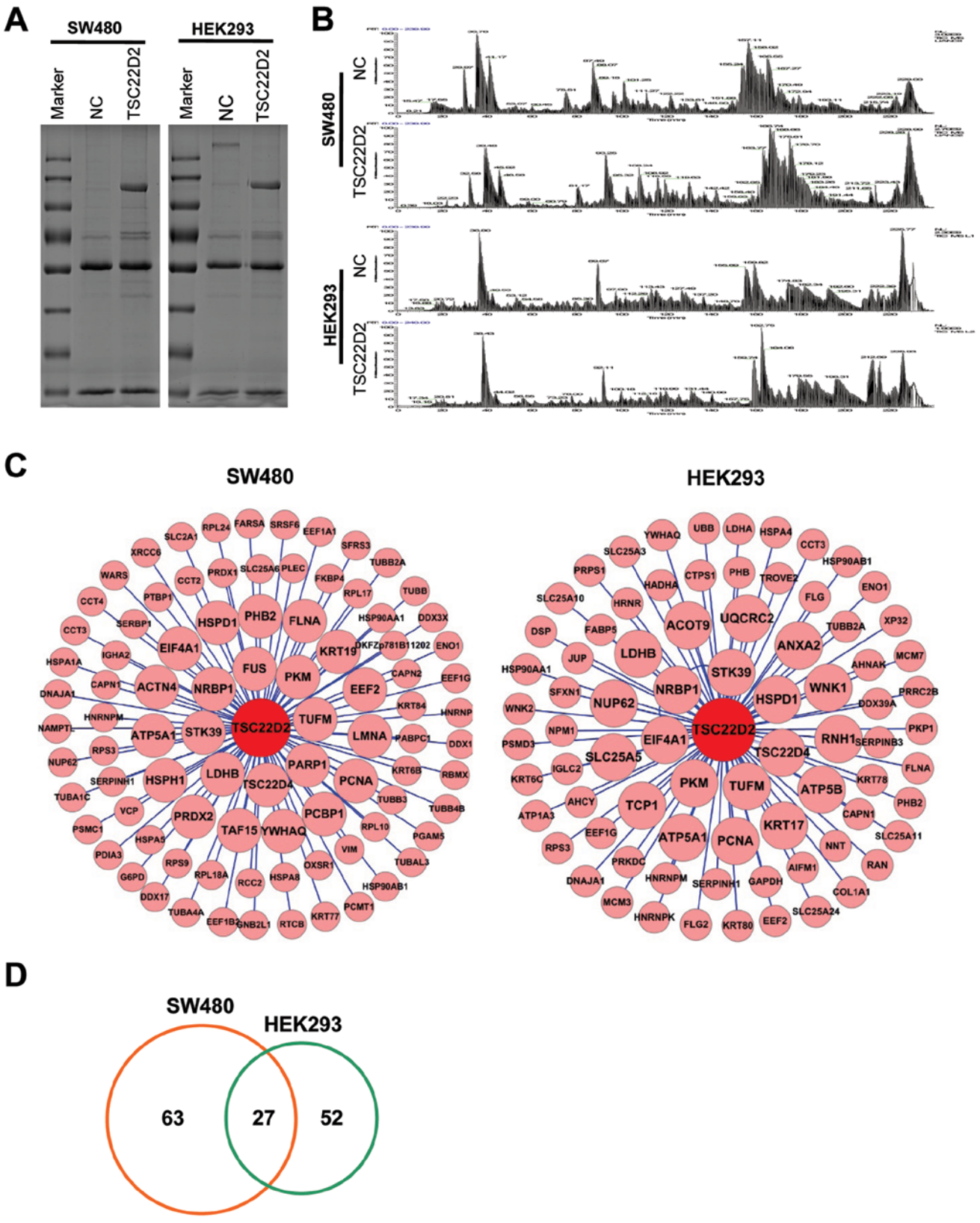

Figure 4. Identification of TSC22D2-interacting proteins using co-IP/MS. (A) SW480 and HEK293 cells transfected with the Flag-TSC22D2 plasmid were extracted and evaluated using immunoprecipitation (IP) with an anti-Flag antibody. The pull-down protein complexes were subjected to SDS-PAGE. (B) The IP-protein complexes were analyzed by LC-MS/MS. Representative images of a TIC from the mass spectrometry analysis. (C) The candidate TSC22D2-interacting proteins identified by IP-MS in SW480 and HEK293 stable cells. (D) There were 27 overlapping TSC22D2 binding proteins identified in between the SW480 and HEK293 cells.

determine whether TSC22D2 and PKM2 co-localize in cells, we performed immunofluorescence staining with anti-Flag and anti-PKM2 antibodies in HEK293 cells. The results revealed that TSC22D2 and PKM2 co-localized primarily in

Table I . TSC22D2-interacting proteins identified in both SW480 and HEK293 cells.

Gene symbol	Description	Confirmed role in cancer
TSC22D2	Fesponse to osmotic stress	
NRBP1	Subcellular trafficking between the endoplasmic reticulum and Golgi apparatus	Potentially plays a suppressive role in tumor progression
TSC22D4	Sequence-specific DNA binding transcription factor activity	
TUFM	Protein translation in mitochondria and oxidative phosphorylation; regulates type I interferon and autophagy	
PKM2	Involved in glycolysis; transcription factor activity	Important for tumor cell proliferation and survival
ATP5A1	A subunit of mitochondrial ATP synthase; involved in energy metabolism	
STK39	A serine/threonine kinase that might function in the cellular stress response pathway	
YWHAQ	Belongs to the 14-3-3 family of proteins, which mediate signal transduction by binding to phospho-serine-containing proteins	Coordinates the regulation of proliferation, survival and metastasis
HSPD1	Putative signaling molecule in the innate immune system; implicated in mitochondrial protein import and macromolecular assembly	Regulates tumor cell apoptosis, survival and metastasis
LDHB	Catalyzes the interconversion of pyruvate and lactate and the concomitant interconversion of NADH and NAD^+ in a post-glycolysis process	A metabolic marker in cancer and is potentially associated with cell growth
PCNA	Cofactor of DNA polymerase delta; DNA damage response	Important for cancer cell proliferation
PHB2	Transcriptional repression; likely to be involved in regulating mitochondrial respiration activity and aging; associated with the cell cycle	Required for cancer cell proliferation, and potentially regulates cell migration
EIF4A1	RNA helicase; translation initiation factor activity; participates in the TGF-β pathway and p70S6K signaling	
ENO1	Functions as a glycolytic enzyme and a transcriptional repressor	Promotes cell proliferation and possesses oncogenic activity
FLNA	A well-characterized actin cross-linking protein; anchors various transmembrane proteins to the actin cytoskeleton and serves as a scaffold for a wide range of cytoplasmic signaling proteins	Has a tumor-promoting effect when localized to the cytoplasm, and suppresses tumor growth and inhibits metastasis when localized to the nucleus
CAPN1	Catalyzes limited proteolysis; involved in ERK signaling and apoptosis	Participates in apoptosis
CCT3	Molecular chaperone; assists in the folding of proteins stimulated by ATP hydrolysis	
DNAJA1	Positive regulation of viral replication; plays a role in protein transport into mitochondria via its role as a co-chaperone; protects cells from apoptosis	Suppresses the anti-apoptosis state in cancer
EEF1G	Translation elongation factor activity; likely to play a role in anchoring the translation complex to other cellular components	

Table I. Continued.

Gene symbol	Description	Confirmed role in cancer
EEF2	Promotes the GTP-dependent translocation of the nascent protein chain from the A-site to the P-site of the ribosome; an essential factor for protein synthesis	Functions as an oncogene in cancer cell growth
HNRNPM	Associated with pre-mRNAs in the nucleus and appears to influence pre-mRNA processing and other aspects of mRNA metabolism and transport	Regulates cell cycle progression, promotes cell growth and invasion; promotes TGFβ-induced EMT and metastasis
HSP90AA1 HSP90AB1	Mediates LPS-induced inflammatory response; molecular chaperone that promotes the maturation, structural maintenance and proper regulation of specific target proteins involved in multiple processes, including cell cycle control and signal transduction	Is involved in cell apoptosis and chemosensitivity Methylated HSP90AB1 accelerates cancer cell proliferation
NUP62	Forms a gateway that regulates the flow of macromolecules between the nucleus and the cytoplasm (involved in nuclear-cytoplasmic transport)	Nup62 knockdown reduces cancer cell growth and viability
RPS3	A component of the 40S small ribosomal subunit; plays a role in the repair of damaged DNA	Regulates cell growth, apoptosis and GLI2-mediated migration and invasion
SERPINH1	A collagen-specific molecular chaperone that plays a role in collagen biosynthesis	Enhances cell growth, migration and invasion
TUBB2A	Key participant in various processes, including mitosis and intracellular transport	

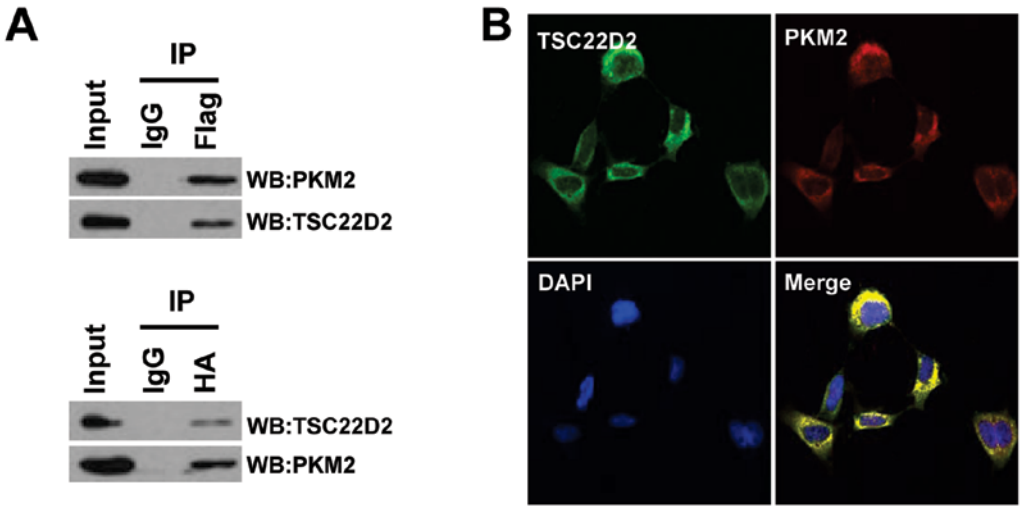

Figure 5. Validation of the interaction between TSC22D2 and PKM2. (A) HEK293T cells transfected with the Flag-TSC22D2 and HA-PKM2 plasmids. A co-IP assay using anti-Flag (TSC22D2) or anti-HA (PKM2) antibodies confirmed that TSC22D2 and PKM2 interact. (B) HEK293T cells stably expressing Flag-TSC22D2 were fixed for immunofluorescence analysis. TSC22D2 was detected using an anti-Flag primary antibody and an Alexa Fluor 488 goat anti-mouse antibody, and PKM2 was detected using an anti-PKM2 primary antibody and an Alexa Fluor 594 goat anti-rabbit antibody. Representative cells from the same field for each experimental group are shown.

the cytoplasm (Pearson's correlation, 0.954) (Fig. 5B). Taken together, these data suggest that TSC22D2 physically associates with PKM2.

TSC22D2 reduces the level of nuclear PKM2 and suppresses the expression of cyclin D1. Accumulating evidence indicates that PKM2 is crucial for aerobic glycolysis and that it provides

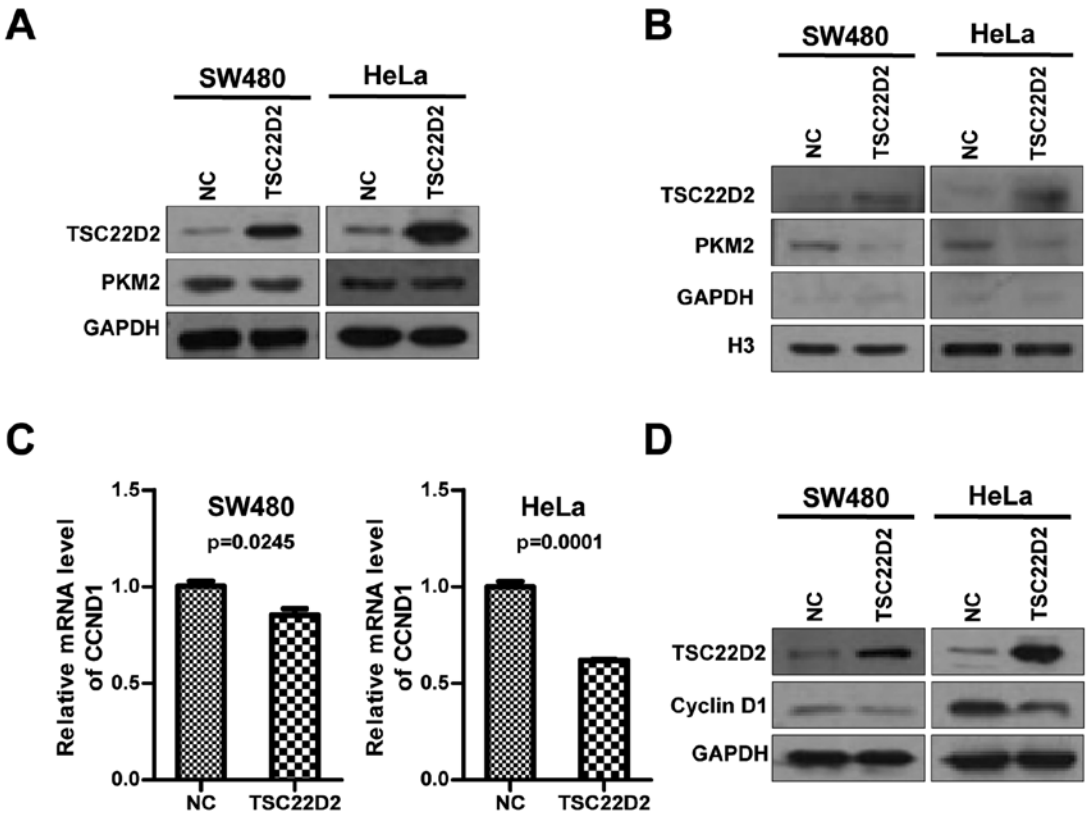

Figure 6. TSC22D2 reduces the level of nuclear PKM2 and suppresses the expression of cyclin D1. (A) The total PKM2 protein levels were analyzed in SW480 and HeLa cells stably overexpressing TSC22D2 using western blot analysis. TSC22D2 did not affect total PKM2 protein levels (B), but it disrupted the nuclear localization of PKM2. (C) The expression levels of cyclin D1 decreased in SW480 and HeLa cells stably overexpressing TSC22D2, as demonstrated by qRT-PCR analysis. (D) The downregulation of cyclin D1 protein levels was confirmed by western blot analysis of cells stably overexpressing TSC22D2.

a growth advantage to tumors (11,12). To determine if the effect of TSC22D2 on cell growth is mediated by PKM2, we evaluated the expression of PKM2 and observed that there were no significant changes in PKM2 expression at the mRNA and protein level in cells overexpressing TSC22D2 (Fig. 6A).

PKM2 predominantly localizes to the cytosol and plays an important role in metabolic functions. Recently, several independent studies demonstrated that PKM2 can translocate to the nucleus and induce the expression of gene products required for tumorigenesis by activating multiple transcription factors (13-18). Thus, we asked whether TSC22D2 could affect the nuclear function of PKM2. A subcellular fractionation analysis was performed, and a slight but significant decrease in the nuclear levels of PKM2 was observed in TSC22D2-overexpressing cells compared with the control cells (Fig. 6B).

Cyclin D1, a key regulator required for the G1/S cell cycle transition, was reported to be a downstream gene of nuclear PKM2 (15,16). Therefore, we next investigated the effect of TSC22D2 on cyclin D1 expression. Intriguingly, TSC22D2 repressed the expression of cyclin D1 at both mRNA and protein levels (Fig. 6C and D), suggesting that TSC22D2 might inhibit cell growth by the influence on nuclear PKM2 and cyclin D1.

Discussion

We previously identified a novel cancer-associated gene, TSC22D2, by performing genome-wide linkage analysis and exome sequencing in samples derived from a multi-cancer family. TSC22D2 is a member of the TSC-22 domain family of proteins that are characterized by a carboxy-terminal leucine zipper and an adjacent TSC-box. However, its role in tumorigenesis remains largely unclear. In this study, we demonstrated that TSC22D2 is expressed at low levels in CRC and that TSC22D2 overexpression significantly inhibited the growth rate of cancer cells. Taken together, these results suggest that TSC22D2 might play a suppressive role in tumorigenesis.

Members of the TSC22 domain family are reported to interact with other proteins to form macromolecular complexes associated with a broad range of biological processes. TSC22D1 (also referred as TSC-22) binds to p53 and protects it from poly-ubiquitination-mediated degradation (2), it can enhance TGF-β signaling by associating with Smad4 (3). TSC22D3 (commonly referred to as GILZ) exhibits multiple biological functions that are dependent on its interaction with other proteins, including NF-κB, Ras and p53 (4-6). TSC22D4 is capable of heterodimerizing with apoptosis-inducing factor (AIF) and might participate in apoptosis (19). However, proteins that interact with TSC22D2 have not been identified.

In this study, we conducted co-IP assays combined with LC-MS/MS approaches to identify TSC22D2-interacting proteins. The results were enriched for proteins associated with the regulation of gene transcription, suggesting that TSC22D2 plays a role in transcription. TSC22 domain proteins have a classic leucine zipper and a TSC-Box structure. The leucine zipper might be a characteristic of a novel

category of DNA binding proteins (20-22) and the TSC-box is essential for nuclear localization and transcriptional activity (23). Based on these observations, TSC22 domain proteins are considered to be putative transcription factors. They primarily localize to the cytoplasm, but in response to specific stimuli, they can also translocate to the nucleus. Previous studies have demonstrated that TSC22D1 can translocate to the nucleus and suppress cell division in response to anti-proliferative stimuli (24,25). TSC22D1 and TSC22D3 transcriptional activity has been previously reported, and the transcriptional activity of TSC22D2 has yet to be further confirmed.

Our analysis revealed that TSC22D2 interacts with multiple proteins associated with metabolism (PKM2, ATP5A1, LDHB and ENO1), the stress response and inflammation (STK39, HSPD1, HSP90AA1 and HSP90AB1), cell proliferation (NRBP1, PKM2, YWHAQ, LDHB, PCNA and PHB2), apoptosis (HSPD1, CAPN1, DNAJA1, HSP90AA1 and RPS3) and migration/metastasis (YWHAQ, HSPD1 and PHB2) (Table I), implying that the function of TSC22D2 in tumor cells might be mediated by these processes. Moreover, the interaction between NRBP1 and TSC22D2 was inadvertently previously reported (26). In addition, TSC22 domain proteins have been shown to homodimerize and heterodimerize with other family members (27). In this study, western blotting and mass spectrometry analyses revealed that TSC22D2 primarily exists as a dimer, but that it might also heterodimerize with TSC22D4.

Given that TSC22D2 was capable of inhibiting the growth of cancer cells, we focused on the PKM2 gene, which was previously reported to be required for tumor growth (7-9). Pyruvate kinase M2 (PKM2) is a pyruvate kinase that regulates the final rate-limiting step of glycolysis by catalyzing the transfer of a phosphate group from phosphoenolpyruvate (PEP) to ADP to generate pyruvate and ATP. PKM2 exhibits active pyruvate kinase activity as well as protein kinase activity that is primarily associated with transcriptional regulation (reviewed in refs. 11,12). Elevated PKM2 expression is currently considered to be a common characteristic of cancers.

PKM2 primarily localized to the cytoplasm. In addition to its well characterized role in glycolysis, PKM2 can translocate to the nucleus to stimulate the activity of multiple transcription factors, including HIF-1, STAT3, β-catenin and Oct-4, thereby increasing the expression of gene products that are required for tumor growth (16-18,28). For example, activation of EGFR in human glioblastoma cells induces the nuclear translocation of PKM2. In addition, the interaction between PKM2 and β-catenin transactivates factors that induce HDAC3 removal from the CCND1 promoter, histone H3 acetylation and cyclin D1 expression (16). An increasing body of evidence indicates that the nuclear translocation of PKM2 promotes the Warburg effect and tumorigenesis (13-18). In this study, we found that TSC22D2 did not regulate the total PKM2 protein levels, but that it decreased the level of nuclear PKM2. Although some studies have suggested that PKM2-interacting proteins impair PKM2 nuclear translocation by altering the balance between its monomer, dimer and tetramer forms or by mediating epigenetic modifications (14,29), further studies are required to confirm the mechanism by which TSC22D2 regulates the nuclear PKM2 level.

In conclusion, this is the first study to report the tumor suppressor role of TSC22D2 in cancer and to identify putative TSC22D2-interacting proteins using interactome analysis. The candidate interactions that we identified provide important clues that will facilitate future studies exploring TSC22D2 functions. The interaction between TSC22D2 and PKM2 may partially account for the growth suppressor function of TSC22D2. It is important to note that further studies of TSC22D2 complexes are required for gaining additional insight into the functions and precise mechanisms associated with TSC22D2 in cancer.

Acknowledgements

We are grateful for the gifts of the HA-PKM2 plasmids from Professor Xianghuo He. We also would like to thank the High Resolution Mass Spectrometry Laboratory of Advanced Research Center in Central South University for the technological assistance in proteomic examinations. This study was supported in part by grants from The National Natural Science Foundation of China (81272298, 81372907, 81301757, 81472531, 81402009, 81572787 and 81528019), the Natural Science Foundation of Hunan Province (14JJ1010 and 2015JJ1022) and the project from Central South University (2013zzts071).

References

1. Li Q, Chen P, Zeng Z, Liang F, Song Y, Xiong F, Li X, Gong Z, Zhou M, Xiang B, *et al*: Yeast two-hybrid screening identified WDR77 as a novel interacting partner of TSC22D2. Tumor Biol (In press).
2. Yoon CH, Rho SB, Kim ST, Kho S, Park J, Jang IS, Woo S, Kim SS, Lee JH and Lee SH: Crucial role of TSC-22 in preventing the proteasomal degradation of p53 in cervical cancer. PLoS One 7: e42006, 2012.
3. Choi SJ, Moon JH, Ahn YW, Ahn JH, Kim DU and Han TH: Tsc-22 enhances TGF-beta signaling by associating with Smad4 and induces erythroid cell differentiation. Mol Cell Biochem 271: 23-28, 2005.
4. Ayroldi E, Migliorati G, Bruscoli S, Marchetti C, Zollo O, Cannarile L, D'Adamio F and Riccardi C: Modulation of T-cell activation by the glucocorticoid-induced leucine zipper factor via inhibition of nuclear factor kappaB. Blood 98: 743-753, 2001.
5. Ayroldi E, Petrillo MG, Bastianelli A, Marchetti MC, Ronchetti S, Nocentini G, Ricciotti L, Cannarile L and Riccardi C: L-GILZ binds p53 and MDM2 and suppresses tumor growth through p53 activation in human cancer cells. Cell Death Differ 22: 118-130, 2015.
6. Ayroldi E, Zollo O, Bastianelli A, Marchetti C, Agostini M, Di Virgilio R and Riccardi C: GILZ mediates the antiproliferative activity of glucocorticoids by negative regulation of Ras signaling. J Clin Invest 117: 1605-1615, 2007.
7. Christofk HR, Vander Heiden MG, Harris MH, Ramanathan A, Gerszten RE, Wei R, Fleming MD, Schreiber SL and Cantley LC: The M2 splice isoform of pyruvate kinase is important for cancer metabolism and tumour growth. Nature 452: 230-233, 2008.
8. Anastasiou D, Yu Y, Israelsen WJ, Jiang JK, Boxer MB, Hong BS, Tempel W, Dimov S, Shen M, Jha A, *et al*: Pyruvate kinase M2 activators promote tetramer formation and suppress tumorigenesis. Nat Chem Biol 8: 839-847, 2012.
9. Hitosugi T, Kang S, Vander Heiden MG, Chung TW, Elf S, Lythgoe K, Dong S, Lonial S, Wang X, Chen GZ, *et al*: Tyrosine phosphorylation inhibits PKM2 to promote the Warburg effect and tumor growth. Sci Signal 2: ra73, 2009.
10. Chen Z, Wang Z, Guo W, Zhang Z, Zhao F, Zhao Y, Jia D, Ding J, Wang H, Yao M, *et al*: TRIM35 interacts with pyruvate kinase isoform M2 to suppress the Warburg effect and tumorigenicity in hepatocellular carcinoma. Oncogene 34: 3946-3956, 2015.
11. Chaneton B and Gottlieb E: Rocking cell metabolism: Revised functions of the key glycolytic regulator PKM2 in cancer. Trends Biochem Sci 37: 309-316, 2012.

12. Luo W and Semenza GL: Emerging roles of PKM2 in cell metabolism and cancer progression. Trends Endocrinol Metab 23: 560-566, 2012.
13. Lv L, Xu YP, Zhao D, Li FL, Wang W, Sasaki N, Jiang Y, Zhou X, Li TT, Guan KL, *et al*: Mitogenic and oncogenic stimulation of K433 acetylation promotes PKM2 protein kinase activity and nuclear localization. Mol Cell 52: 340-352, 2013.
14. Yang W, Zheng Y, Xia Y, Ji H, Chen X, Guo F, Lyssiotis CA, Aldape K, Cantley LC and Lu Z: ERK1/2-dependent phosphorylation and nuclear translocation of PKM2 promotes the Warburg effect. Nat Cell Biol 14: 1295-1304, 2012.
15. Yang W, Xia Y, Hawke D, Li X, Liang J, Xing D, Aldape K, Hunter T, Alfred Yung WK and Lu Z: PKM2 phosphorylates histone H3 and promotes gene transcription and tumorigenesis. Cell 150: 685-696, 2012.
16. Yang W, Xia Y, Ji H, Zheng Y, Liang J, Huang W, Gao X, Aldape K and Lu Z: Nuclear PKM2 regulates β-catenin transactivation upon EGFR activation. Nature 480: 118-122, 2011.
17. Luo W, Hu H, Chang R, Zhong J, Knabel M, O'Meally R, Cole RN, Pandey A and Semenza GL: Pyruvate kinase M2 is a PHD3-stimulated coactivator for hypoxia-inducible factor 1. Cell 145: 732-744, 2011.
18. Lee J, Kim HK, Han YM and Kim J: Pyruvate kinase isozyme type M2 (PKM2) interacts and cooperates with Oct-4 in regulating transcription. Int J Biochem Cell Biol 40: 1043-1054, 2008.
19. Lim J, Hao T, Shaw C, Patel AJ, Szabó G, Rual JF, Fisk CJ, Li N, Smolyar A, Hill DE, *et al*: A protein-protein interaction network for human inherited ataxias and disorders of Purkinje cell degeneration. Cell 125: 801-814, 2006.
20. Landschulz WH, Johnson PF and McKnight SL: The leucine zipper: A hypothetical structure common to a new class of DNA binding proteins. Science 240: 1759-1764, 1988.
21. Kouzarides T and Ziff E: Leucine zippers of fos, jun and GCN4 dictate dimerization specificity and thereby control DNA binding. Nature 340: 568-571, 1989.
22. Busch SJ and Sassone-Corsi P: Dimers, leucine zippers and DNA-binding domains. Trends Genet 6: 36-40, 1990.
23. Hashiguchi A, Hitachi K, Inui M, Okabayashi K and Asashima M: TSC-box is essential for the nuclear localization and antiproliferative effect of XTSC-22. Dev Growth Differ 49: 197-204, 2007.
24. Hino S, Kawamata H, Uchida D, Omotehara F, Miwa Y, Begum NM, Yoshida H, Fujimori T and Sato M: Nuclear translocation of TSC-22 (TGF-beta-stimulated clone-22) concomitant with apoptosis: TSC-22 as a putative transcriptional regulator. Biochem Biophys Res Commun 278: 659-664, 2000.
25. Nakamura M, Kitaura J, Enomoto Y, Lu Y, Nishimura K, Isobe M, Ozaki K, Komeno Y, Nakahara F, Oki T, *et al*: Transforming growth factor-β-stimulated clone-22 is a negative-feedback regulator of Ras/Raf signaling: Implications for tumorigenesis. Cancer Sci 103: 26-33, 2012.
26. Gluderer S, Brunner E, Germann M, Jovaisaite V, Li C, Rentsch CA, Hafen E and Stocker H: Madm (Mlf1 adapter molecule) cooperates with Bunched A to promote growth in Drosophila. J Biol 9: 9, 2010.
27. Kester HA, Blanchetot C, den Hertog J, van der Saag PT and van der Burg B: Transforming growth factor-beta-stimulated clone-22 is a member of a family of leucine zipper proteins that can homo- and heterodimerize and has transcriptional repressor activity. J Biol Chem 274: 27439-27447, 1999.
28. Gao X, Wang H, Yang JJ, Liu X and Liu ZR: Pyruvate kinase M2 regulates gene transcription by acting as a protein kinase. Mol Cell 45: 598-609, 2012.
29. Wang HJ, Hsieh YJ, Cheng WC, Lin CP, Lin YS, Yang SF, Chen CC, Izumiya Y, Yu JS, Kung HJ, *et al*: JMJD5 regulates PKM2 nuclear translocation and reprograms HIF-1α-mediated glucose metabolism. Proc Natl Acad Sci USA 111: 279-284, 2014.